Rev. Adv. Mater. Sci. 37 (2014) 83-89

EQUILIBRIUM DISLOCATION STRUCTURES AT GRAIN BOUNDARIES IN SUBSURFACE AREAS OF POLYCRYSTALLINE GRAPHENE AND ULTRAFINE-GRAINED METALS

Ya.V. Konakov[1,3], I.A. Ovid'ko[1,2,3] and A.G. Sheinerman[1,2,3]

[1]Institute of Problems of Mechanical Engineering, Russian Academy of Sciences, Bolshoj 61, Vasil. Ostrov, St. Petersburg 199178, Russia
[2]Department of Mathematics and Mechanics, St. Petersburg State University, Universitetskii pr. 28, Staryi Peterhof, St. Petersburg 198504, Russia
[3]Research Laboratory for Mechanics of New Nanomaterials, St. Petersburg State Polytechnical University, St. Petersburg 195251, Russia

Received: March 1, 2014

Abstract. A theoretical model is suggested which describes distribution of grain boundary (GB) dislocations at GBs located in subsurface areas of polycrystalline graphene and ultrafine-grained metals. Within the suggested model, spatial distribution of GB dislocations – basic structural units of GBs – are theoretically revealed as those depending on the presence of triple junction disclinations in polycrystalline graphene and ultrafine-grained metals.

1. INTRODUCTION

Polycrystalline graphene sheets and ultrafine-grained metals contain grain boundaries (GBs) as inevitable structural defects strongly influencing the unique mechanical and functional properties of these advanced materials; see, e.g., reviews [1-11]. For instance, superior tensile strength of graphene sheets dramatically degrades due to the effects of GBs [5,6,12–19], and their geometry/curvature can be effectively controlled by GB structures [5,20]. Ultrafine-grained metals are specified by large amounts of GBs which crucially affect strength and ductility as well as the functional properties of these metals [7–11,21–24]. In both polycrystalline graphene and ultrafine-grained metals in their as-fabricated states, GBs typically have rather irregular structures that typically contain special rotational defects called partial disclinations; for details, see a discussion in paper [25] and references therein. Also, in the subsurface areas of these advanced materials, the free surface effects operate which influence GB structures and thereby properties of both polycrystalline graphene and ultrafine-grained metals. In this context, it is very interesting to understand the combined effects of the free surface and the presence of disclinations on GB structures in polycrystalline graphene and ultrafine-grained metals. The main aim of this paper is to theoretically describe "equilibrium" structures of initially disclinated GBs in the subsurface areas of polycrystalline graphene and ultrafine-grained metals.

2. DISLOCATION STRUCTURES OF DISCLINATED GRAIN BOUNDARIES IN SUBSURFACE AREAS OF POLYCRYSTALLINE GRAPHENE SHEETS

Let us consider a polycrystalline graphene sheet containing grains divided by GBs (Fig. 1a). Let us

Corresponding author: Ilya Ovid'ko, e-mail: ovidko@nano.ipme.ru

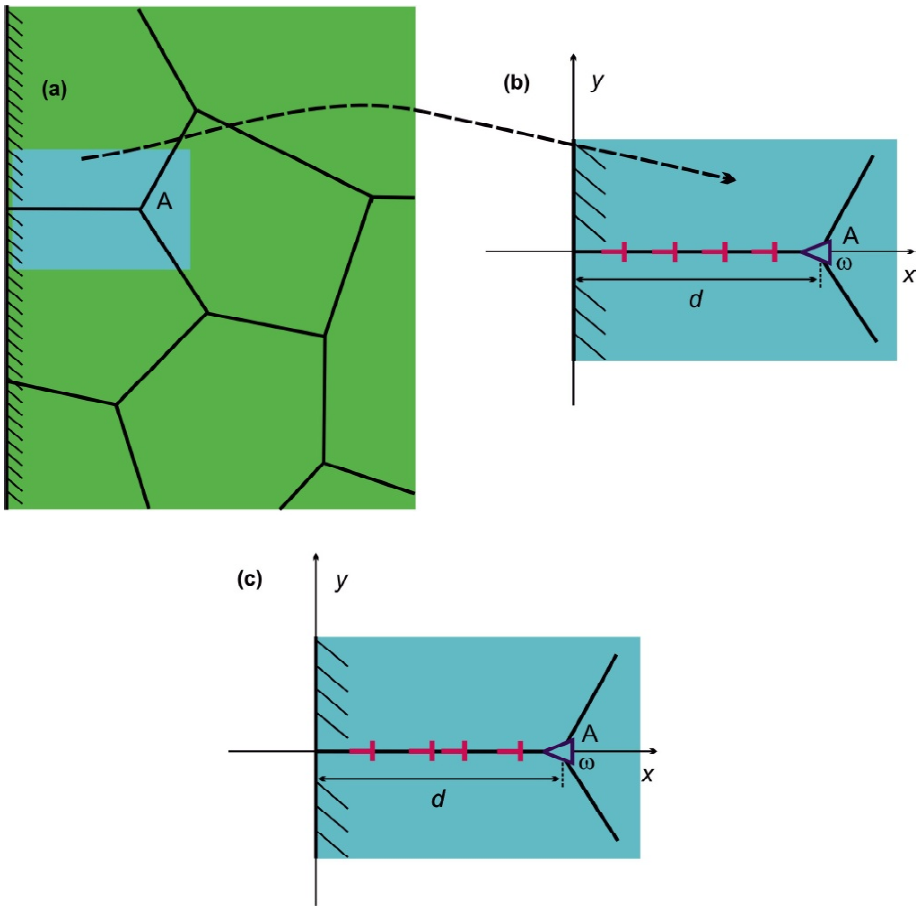

Fig. 1. (Color online) Grain boundaries in subsurface area of graphene. (a) Subsurface area of graphene. General view. (b) Magnified inset highlights a subsurface grain boundary containing a regular wall of perfect edge dislocations and a wedge disclination of strength ω at the triple junction A. (c) Magnified inset highlights a subsurface grain boundary containing perfect edge dislocations at their equilibrium positions and a wedge disclination of strength ω at the triple junction A.

examine in more detail a symmetric low-angle GB that extends between a triple junction of GBs and the lateral free surface of graphene (Fig. 1b). We assume that the examined GB has the length d, is normal to the lateral graphene surface and contains a regular wall of perfect edge dislocations with the Burgers vectors b. Also, a wedge disclination of strength ω is located at a triple junction that bounds the examined GB.

In the Cartesian coordinate system (x,y) shown in Fig. 1b, the GB lies at the line $y = 0$, while the dislocations Burgers vectors b are directed along the y-axis. Every dislocation at the GB is under the action of the force exerted by other dislocations and the disclination. Let us assume that under the action of this force, dislocations in the GB climb along it until they either have reached their equilibrium positions or approached the free surface (Fig. 1c).

Let us calculate the equilibrium positions of dislocations after their climb along the GB. To do so, we come from the discrete distribution of perfect dislocations with the Burgers vectors $\boldsymbol{b}$ to their continuous distribution characterized by the linear dislocation density $\rho(x)$. We define the dislocation density $\rho(x)$ as $\rho(x) = db_y/dx$. In turn, for convenience of our calculations, we come from the continuous dislocation distribution to the discrete distribution of virtual dislocations with fixed positions but varying magnitudes of the Burgers vectors. Within our model, the virtual dislocations are located at the points $x = x_k = (k - 1/2)d/N$ (where k is the number of a specified dislocation, and N is the total number of dislocations; $k = 1,\ldots N$) with the fixed separation d/N, while their Burgers vectors $\boldsymbol{b}_k$ are directed along the y-axis and characterized by the projections $b_{ky} = \rho(x_k)d/N$. In the initial state with the GB containing a regular dislocation wall, the value of b_{ky} is constant for any k and equal to B/N, where B is the total magnitude of the dislocations Burgers vectors. At the same time, the climb of the real perfect dis-

locations along the GB is modeled as changes of the projections b_{ky} of the Burgers vectors of the "fixed" virtual dislocations, that correspond to the variations of the dislocation density $\rho(x)$.

In order to calculate the equilibrium distribution of subsurface dislocations, we calculate the total energy of the examined defects (dislocations and the disclination). The energy W is given by the sum of the proper energies of the defects and the energies of their elastic interaction. The expression for the energy W is cast using the expressions [26,27] for the stress fields of dislocations and a disclination located near a flat free surface as follows:

$$W = D\sum_{k=1}^{N}\sum_{i=k+1}^{N} b_{iy}\, b_{ky}\left(\ln\left|\frac{x_i + x_k}{x_i - x_k}\right| - \frac{2x_i x_k}{(x_i + x_k)^2}\right) + \frac{D}{2}\sum_{k=1}^{N} b_{ky}^2\left(\ln\frac{2x_k}{b} + \frac{1}{2}\right) +$$
$$D\omega\sum_{k=1}^{N} b_{ky}\left((d - x_k)\ln\frac{d - x_k}{d + x_k} - \frac{2x_k d}{x_k + d}\right) + W^{\Delta}. \qquad (1)$$

In formula (1), $D = E/(4\pi)$, E is the Young modulus of graphene, b is the interatomic spacing in monolayer graphene sheets, and W^{Δ} is the proper energy of the disclination.

Let us suppose that dislocations in the examined GB can enter the lateral graphene surface but cannot nucleate at this surface. This assumption reflects the fact that there is a large energy barrier for dislocation generation at the free surface, whereas disappearance of a dislocation at the free surface is a low-barrier process. The assumption means that the direction of the dislocation Burgers vectors cannot reverse, and the relation $b_{ky} \geq 0$ is valid for any dislocation number k. Also, first, we consider the case where dislocations do not enter the lateral graphene surface and, as a result, the total magnitude B of the dislocations Burgers vectors does not change, that is,

$$\sum_{k=1}^{N} b_{ky} = B. \qquad (2)$$

In this case, the equilibrium values of b_{ky} correspond to the conditional minimum of the energy W, with relation (2) taken into account. In order to calculate the equilibrium values of b_{ky} that correspond to the conditional minimum of the energy W, we introduce the Lagrange function

$$L = W + \lambda\left(\sum_{k=1}^{N} b_{ky} - B\right). \qquad (3)$$

The conditional minimum of the energy W (with relation (2) taken into account) corresponds to the absolute minimum of the function L. This means that the quantities b_{ky} are determined from both Eq. (2) and the relations $\partial W/\partial b_{ky} = 0$ ($k = 1,\ldots N$).

Substitution of the latter relations to formula (3), in combination with formula (2), yields the following system of the linear equations for b_{ky}:

$$\begin{cases} \displaystyle\sum_{i=k+1}^{N} b_{iy}\left(\ln\left|\frac{x_i + x_k}{x_i - x_k}\right| - \frac{2x_i x_k}{(x_i + x_k)^2}\right) + b_{ky}\left(\ln\frac{2x_k}{b} + \frac{1}{2}\right) + \\ \omega\left((d - x_k)\ln\dfrac{d - x_k}{d + x_k} - \dfrac{2x_k d}{x_k + d}\right) + \lambda = 0 \qquad , \ k = 1,\ldots,N, \\ \displaystyle\sum_{k=1}^{N} b_{ky} = B. \end{cases} \qquad (4)$$

It should be noted that system of Eqs. (4) has a single solution, and, as a consequence, the energy W has a single minimum. The analysis demonstrates that this minimum is sometimes reached at negative values of the projections b_{ky} of some dislocation Burgers vectors. In other words, the condition $b_{ky} \geq 0$ may not be fulfilled for some (closest to the surface) dislocations. Therefore, in the calculation of the equilibrium density of dislocations, we employ the following iteration procedure. If the value of b_{1y}, obtained from the solution of the system of (N+1) equations given by formulae (4), becomes negative, we put $b_{1y} = 0$ and solve

the system of N equations, obtained by substitution of the relation $b_{1y} = 0$ to system (4) and elimination of the equation for $k = 1$, corresponding to the condition $\partial L/\partial b_{1y} = 0$, from this system. If the value of b_{2y}, obtained from the solution of the new system of equations, becomes negative, we put $b_{2y} = 0$ and solve the system of (N-1) equations, obtained by substitution of the relations $b_{1y} = 0$ and $b_{2y} = 0$ to system (4) and elimination of the equations for $k = 1$ and $k = 2$, corresponding to the conditions $\partial L/\partial b_{1y} = 0$ and $\partial L/\partial b_{2y} = 0$, from this system. The above iteration procedure is repeated until the relation $b_{ky} \geq 0$ has been met for any k. After that, using the equilibrium values of b_{ky}, we calculate the dislocation density $\rho(x)$. For definiteness, we also set $\omega > 0$.

It is worth noting that the above iterative procedure postulates the possibility for the formation of a dislocation-free region near the lateral graphene surface, where the projections b_{ky} of the dislocation Burgers vectors $\boldsymbol{b}_k$ are set equal to zero. To confirm the above iterative procedure, we carried out additional calculations by an alternative method where all the Burgers vectors projections b_{ky} are set equal to B/N and the energy W is minimized with respect to the dislocation coordinates x_k. The calculations using this alternative method provided nearly the same dependences $\rho(x)$ as the above iteration procedure and confirmed the possibility for the formation of a dislocation-free region near the lateral graphene surface.

The analysis of the obtained dependences $\rho(x)$ has demonstrated that one can distinguish the following three different cases: $\rho_0/\omega > 1$, $\rho_0/\omega = 1$, and $\rho_0/\omega < 1$, where $\rho_0 = B/d$ is the initial dislocation density. According to the theory of defects in solids [27], in the case of $\rho_0/\omega = 1$, the dislocation wall is equivalent to the wedge disclination of strength $-\omega$, located at the triple junction that bounds the examined GB. This implies that such a dislocation wall creates stresses which completely compensate for the stresses created by the wedge disclination of strength w. In this situation, the initial distribution of dislocations with the constant density $\rho(x) = \omega$ corresponds to the energy minimum, and dislocations do not climb along the GB.

The dependences of the dislocation density ρ on the coordinate x in the cases $\rho_0/\omega > 1$ and $\rho_0/\omega < 1$ are plotted in Figs. 2a and 2b, respectively, for various values of the parameters B/d and ω. As it follows from Fig. 2a, in the case of $\rho_0/\omega > 1$, the dislocation density ρ that corresponds to the minimum of the energy W, for a constant specified magnitude B of the total dislocation Burgers vector, increases near the lateral graphene surface. Our analysis demonstrates that, for such a dislocation distribution, the dislocations located near the lateral free surface are attracted to this surface and enter it. As a corollary, the magnitude of the total dislocation Burgers vector decreases. The process of dislocation motion to the lateral free surface occurs until the average dislocation density has become equal to the disclination strength, that is, until the relation $B/d = \omega$ has become valid. When the latter relation is met, the dislocations left in the GB climb to their equilibrium positions that correspond to the constant dislocation density $\rho(x) = \omega$.

Fig. 2b illustrates the equilibrium dislocation distribution at the GB in the case of $\rho_0/\omega < 1$. As it is seen in Fig. 2b, in this case, a dislocation-free region forms near the lateral graphene surface. With an increase of the distance from the lateral free surface, the dislocation density ρ increases. At the same time, near the triple junction containing the disclination, the dislocation density again decreases. The analysis has demonstrated that the dislocation distribution shown in Fig. 2b is equilibrium, and the dislocations do not enter the lateral surface. Thus, in the case of $\rho_0/\omega < 1$, dislocation climb along the subsurface GB without entering the lateral graphene surface.

3. DISLOCATION STRUCTURES OF DISCLINATED GRAIN BOUNDARIES IN SUBSURFACE AREAS OF ULTRAFINE-GRAINED METALS

The previously considered model of dislocation structures at initially disclinated low-angle GBs in subsurface areas of graphene sheets can also be extended to the case of subsurface areas of ultrafine-grained metals. In this case, GB dislocations and disclinations represent linear defects at the 2D GB, and the ultrafine-grained metal is modeled as a semi-infinite solid in the plane strain state. In the discussed case of a semi-infinite three-dimensional solid, all the above formulae remain valid if one replaces the Young modulus E by $E/(1 - \nu^2)$, where ν is Poisson's ratio. However, since the equilibrium dislocation density ρ (determined solely by system of Eqs. (4) that do not incorporate elastic constants as parameters) does not depend on the elastic moduli E and ν, it does not change in the case of ultrafine-grained metals. Besides, since ρ does not depend on E and ν, the dependences $\rho(x)$ are the same for any ultrafine-grained metal.

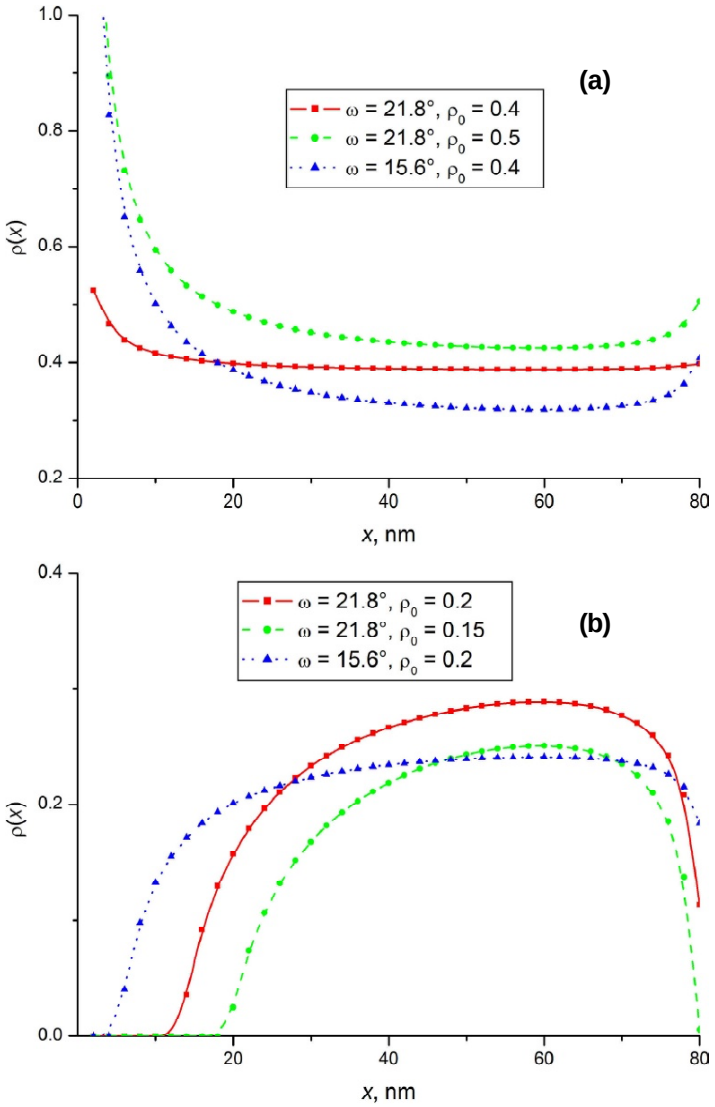

Fig. 2. (Color online) Dependences of the equilibrium density $\rho(x)$ of dislocations at a subsurface grain boundary with the length d = 80 nm in graphene on the coordinate x, for N = 40. (a) $\rho_0/\omega > 1$. (b) $\rho_0/\omega < 1$.

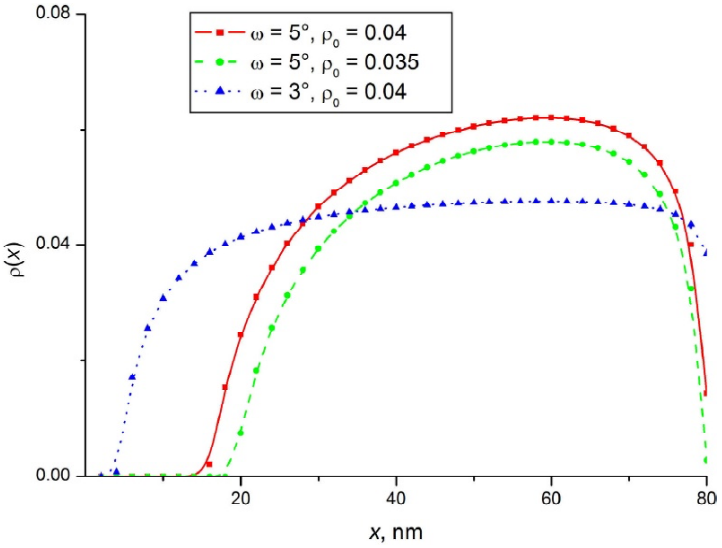

Fig. 3. (Color online) Dependences of the equilibrium density $\rho(x)$ of dislocations at a subsurface grain boundary with the length d = 80 nm in an ultrafine-grained metal on the coordinate x, for N = 40, $\rho_0/\omega < 1$.

Fig. 3 illustrates the dependences $\rho(x)$ specifying GB dislocation structures in ultrafine-grained metals in the case of $\rho_0/\omega < 1$, for various values of the parameters ω and ρ_0. From Figs. 2 and 3 one can see the qualitative similarity of the character of dislocation distributions in subsurface GBs in graphene and ultrafine-grained metals.

4. CONCLUDING REMARKS

In this paper, a theoretical model was suggested describing structural transformations of GBs located in the subsurface areas of polycrystalline graphene and ultrafine-grained metals. We considered GBs which are perpendicular to free surfaces and have wedge disclinations at their triple junctions with neighboring GBs (Fig. 1). Within the suggested model, the transformations occur through GB dislocation climb processes driven by decrease in the elastic energy of GB defect ensemble. It has been theoretically revealed that the structural transformations of GBs in polycrystalline graphene and ultrafine-grained metals can result in either spatially inhomogeneous or homogeneous distributions of GB dislocations, depending on the geometric parameters of GB dislocation configurations and triple junction disclinations. In doing so, one distinguishes three cases: $\rho_0/\omega > 1$, $\rho_0/\omega = 1$, and $\rho_0/\omega < 1$, where $\rho_0 = B/d$ is the initial dislocation density, and ω is the disclination strength. In the case of $\rho_0/\omega = 1$, the initial distribution of dislocations with the constant density $\rho(x) = \omega$ corresponds to the energy minimum, and dislocations do not climb along the GB. In the case of $\rho_0/\omega = 1$, the process of dislocation motion to the lateral free surface occurs until the average dislocation density has become equal to the disclination strength, and the dislocations left in the GB climb to their equilibrium positions that correspond to the constant dislocation density $\rho(x) = \omega$. In the case of $\rho_0/\omega < 1$, equilibrium GB dislocation distributions are spatially inhomogeneous (see Figs. 2b and 3). Such spatially inhomogeneous distributions of GB dislocations at GBs are rather unusual and serve as specific structural features of GBs located near free surfaces in polycrystalline graphene and ultrafine-grained metals. These specific structural features of GBs are expected to significantly influence the properties of the subsurface areas of polycrystalline graphene and ultrafine-grained metals.

ACKNOWLEDGEMENTS

This work was supported, in part, (for Ya.V.K.) by the Russian Foundation of Basic Research (grant 12-01-00291-a), (for I.A.O.) by St. Petersburg State University research grant 6.37.671.2013, and (for A.G.S.) by the Russian Ministry of Education and Science (Grant 14.B25.31.0017).

REFERENCES

[1] K.S. Novoselov, A.K. Geim, S.V. Morozov, D. Jiang, Y. Zhang, S.V. Dubonos, I.V. Grigorieva and A.A. Firsov // *Science* **306** (2004) 666.
[2] A.K. Geim and K.S. Novoselov // *Nature Mater*. **6** (2007) 183.
[3] A.K. Geim // *Science* **324** (2009) 1530.
[4] A.H. Castro Nero, F. Guinea, N.M. R. Peres, K.S. Novoselov and A.K. Geim // *Rev. Mod. Phys.* **81** (2009) 109.
[5] I.A. Ovid'ko // *Rev. Adv. Mater. Sci*. **30** (2012) 201.
[6] I.A. Ovid'ko // *Rev. Adv. Mater. Sci*. **34** (2013) 1.
[7] R.Z. Valiev // *Nature Mater.* **3** (2004) 511.
[8] I.A. Ovid'ko and T.G. Langdon // *Rev. Adv. Mater. Sci*. **30** (2012) 103.
[9] R.Z. Valiev, I. Sabirov, A.P. Zhilyaev and T.G. Langdon // *JOM* **64** (2012) 1134.
[10] Y. Estrin and A. Vinogradov // *Acta Mater*. **61** (2013) 782.
[11] T. Sakai, A. Belyakov, R. Kaibyshev, H. Miura and J.J. Jonas // *Prog. Mater. Sci*. **60** (2014) 130.
[12] P.Y. Huang, C.S. Ruiz-Vargas, A.M. van der Zande, W.S. Whitney, M.P. Levendorf, J.W. Kevek, S. Garg, J.S. Alden, C.J. Hustedt, Y. Zhu, J. Park, P.L. McEuen and D.A. Muller // *Nature* **469** (2011) 389.
[13] C.S. Ruiz-Vargas, H.L. Zhuang, P.Y. Huang, A.M. van der Zande, S. Garg, P.L. McEuen, D.A. Miller, R.C. Hennig and J. Park // *Nano Lett*. **11** (2011) 2259.
[14] Y. Wei, J. Wu, H. Yin, X. Shi, R. Yang and M. Dresselhaus // *Nature Mater*. **11** (2012) 759.
[15] R. Grantab, V.B. Shenoy, R.S. Ruoff // *Science* **330** (2010) 946.
[16] T.-H. Liu, C.-W. Pao, C.-C. Chang // *Carbon* **50** (2012) 3465.
[17] Y.I. Jhon, S.-E. Zhu, J.-H. Ahn and M.S. Jhon // *Carbon* **50** (2012) 3708.
[18] J. Zhang, J. Zhao, J. Lu and *ACS Nano* **6** (2012) 2704.
[19] I.A. Ovid'ko and A.G. Sheinerman // *J. Phys. D: Appl. Phys.* **46** (2013) 345305.

[20] I.A. Ovid'ko // *Rev. Adv. Mater. Sci*. **32** (2012) 1.
[21] I.A. Ovid'ko and A.G. Sheinerman // *Rev. Adv. Mater. Sci*. **35** (2013) 48.
[22] R.Z. Valiev, M.Yu. Murashkin and I. Sabirov // Scr. Mater. **76** (2014) 13.
[23] I.A. Ovid'ko and N.V. Skiba // Scr. Mater. **71** (2014) 33.
[24] I.A. Ovid'ko, A.G. Sheinerman and R.Z. Valiev // Scr. Mater. **76** (2014) 45.
[25] Ya.G. Konakov, I.A. Ovid'ko and A.G. Sheinerman // *Rev. Adv. Mater. Sci*. **35** (2013) 104.
[26] J.P. Hirth and J. Lothe, *Theory of Dislocations* (Wiley, New York, 1982).
[27] A.E Romanov and V.I. Vladimirov, In: *Dislocations in Solids*, ed. by F.R.N. Nabarro (North-Holland, Amsterdam).